

Citation for published version:

Sharpe, J, Bimbo, N, Ting, V, Burrows, A, Jiang, D & Mays, T 2013, 'Supercritical hydrogen adsorption in nanostructured solids with hydrogen density variation in pores', *Adsorption*, vol. 19, no. 2-4, pp. 643-652. <https://doi.org/10.1007/s10450-013-9487-6>

DOI:

[10.1007/s10450-013-9487-6](https://doi.org/10.1007/s10450-013-9487-6)

Publication date:

2013

Document Version

Peer reviewed version

[Link to publication](#)

The original publication is available at www.springerlink.com

University of Bath

Alternative formats

If you require this document in an alternative format, please contact:
openaccess@bath.ac.uk

General rights

Copyright and moral rights for the publications made accessible in the public portal are retained by the authors and/or other copyright owners and it is a condition of accessing publications that users recognise and abide by the legal requirements associated with these rights.

Take down policy

If you believe that this document breaches copyright please contact us providing details, and we will remove access to the work immediately and investigate your claim.

Supercritical hydrogen adsorption in nanostructured solids with hydrogen density variation in pores

Jessica E. Sharpe

*EPSRC Doctoral Training Centre, Centre for Sustainable Chemical Technologies,
Department of Chemical Engineering, University of Bath, BA2 7AY, United
Kingdom.*

Nuno Bimbo, Valeska P. Ting

*Department of Chemical Engineering, University of Bath, Bath, BA2 7AY, United
Kingdom.*

Andrew D. Burrows, Dongmei Jiang

Department of Chemistry, University of Bath, Bath, BA2 7AY, United Kingdom.

Timothy J. Mays

*Room 3.02, 9W Building, Department of Chemical Engineering, University of
Bath, Bath, BA2 7AY, United Kingdom.*

phone: +44 (0) 1225 386 528

fax: +44 (0) 1225 385 710

T.J.Mays@bath.ac.uk

1
2
3
4
5
6
7
8
9
10
11
12
13
14
15
16
17
18
19
20
21
22
23
24
25
26
27
28
29
30
31
32
33
34
35
36
37
38

Abstract:

Experimental excess isotherms for the adsorption of gases in porous solids may be represented by mathematical models that incorporate the total amount of gas within a pore, a quantity which cannot easily be found experimentally but which is important for calculations for many applications, including adsorptive storage. A model that is currently used for hydrogen adsorption in porous solids has been improved to include a more realistic density profile of the gas within the pore, and allows calculation of the total amount of adsorbent. A comparison has been made between different Type I isotherm equations embedded in the model, by examining the quality of the fits to hydrogen isotherms for six different nanoporous materials. A new Type I isotherm equation which has not previously been reported in the literature, the Unilan- b equation, has been derived and has also been included in this comparison study. These results indicate that while some Type I isotherm equations fit certain types of materials better than others, the Tóth equation produces the best overall quality of fit and also provides realistic parameter values when used to analyse hydrogen sorption data for a model carbon adsorbent.

Keywords:

Hydrogen adsorption, porous solids, isotherm equations

Abbreviations:

MOF: metal-organic framework; PIM: polymer of intrinsic microporosity; m_E : excess mass of hydrogen; v_P : pore volume; ρ_B : bulk density; m_A^{\max} : limiting maximum uptake; θ_A : fractional filling; wt%: weight percent; P : absolute pressure; b : affinity parameter; Q : enthalpic factor; b_0 : pre-exponential factor; R : molar gas constant; T : absolute temperature; bdc: benzene-1,4-dicarboxylate; MIL: Matériaux de l'Institut Lavoisier; BET: Brunauer, Emmett and Teller; $m_{B(A)}$: bulk hydrogen within the adsorbate; m_A : absolute uptake; m_P : total uptake; ρ_A : adsorbate density; v_A : adsorbate volume; M : molar mass; Z : compressibility factor; NIST: National Institute of Standards and Technology; $b_{(T)}$: Tóth affinity parameter; $c_{(T)}$: Tóth heterogeneity parameter; $RMSR$: root mean square residual; RSS : residual sum of squares; i : an index for the data; y_i : data value; \hat{y}_i : function value; DOF : degrees of freedom; n : number of data points; p : number of parameters; b_1 : minimum value of b in a uniform distribution; b_2 : maximum value of b in a uniform

1 distribution; Q_1 : minimum value of Q in a uniform
 2 distribution; Q_2 : maximum value of Q in a uniform
 3 distribution; $\theta(P, h)$: local isotherm; h : heterogeneity
 4 parameter; w : substitution variable; $b_{(L)}$: Langmuir
 5 affinity parameter; $b_{(S)}$: Sips affinity parameter; $m_{(S)}$:
 6 Sips heterogeneity parameter; $b_{(GF)}$: Generalised
 7 Freundlich affinity parameter; q : Generalised
 8 Freundlich heterogeneity parameter; $b_{(JF)}$: Jovanović-
 9 Freundlich affinity parameter; $c_{(JF)}$: Jovanović-
 10 Freundlich heterogeneity parameter; α : Dubinin-
 11 Astakhov enthalpic factor; β : Dubinin-Astakhov
 12 entropic factor; $m_{(DA)}$: adjustable parameter within the
 13 Dubinin-Astakhov equation; P_0 : vapour pressure;
 14 GCMC: grand-canonical Monte Carlo.
 15

16 **1. Introduction**

17 Hydrogen shows great potential as an energy store; it is ubiquitous in the
 18 environment (in water and biomass), it can be sustainably produced, has the
 19 highest energy per unit mass of any chemical fuel, and only water is produced as a
 20 by-product when releasing stored energy via heat engines or electrochemical
 21 devices such as fuel cells. However, a major issue with using hydrogen as an
 22 energy store is its very low energy density per unit volume. The density needs to
 23 be vastly increased to make it commercially viable, especially in applications
 24 where low mass, low volume stores are required, for example in light-duty land
 25 vehicles or to minimise plant footprints for static energy stores. Physisorption of
 26 molecular hydrogen (H_2) in nanoporous materials is one promising method of
 27 doing this and may improve on the conventional storage of liquid H_2 at low
 28 temperature (< 33 K) or high pressure gas (up to 70 MPa). Adsorptive storage
 29 does not require a large energy input to recover the hydrogen from the adsorbent,
 30 unlike chemisorption, due to the relatively weak interaction between the adsorbent
 31 and the hydrogen, however, because of these weak interactions, low temperatures
 32 are required to store large quantities.
 33

34 Materials that are commonly considered for gas storage include metal-organic
 35 frameworks (MOFs) (James 2003), zeolites (Bekkum 2001), activated carbons

(Ströbel et al. 2006) and polymers of intrinsic microporosity (PIMs) (McKeown, Budd 2006). Analysis of these systems using adsorption models is very important for two main reasons. Firstly, models may be used to calculate the total amount of hydrogen within the system at any pressure and temperature (which cannot easily be measured experimentally) in order to compare the suitability of different materials for hydrogen storage. Secondly, models may be used to better understand fundamental aspects of the hydrogen adsorption process and hence guide materials design and selection, for example by finding the optimum pore sizes required to store the maximum quantity of hydrogen. The models must be framed to represent the excess mass of hydrogen, m_E , in order to fit to the Gibbs' excess isotherms obtained experimentally using volumetric or gravimetric gas sorption analysers. The excess refers to the additional amount of hydrogen in the pore as a result of the interactions between the hydrogen and the surface of the material. The basic model that is commonly utilized for hydrogen adsorption (Equation 1) (Purewal et al. 2012; Czerny et al. 2005; Bimbo et al. 2011) assumes a uniform hydrogen density profile within the pore, and includes terms for the specific open pore volume, v_P , the mass density of the bulk hydrogen, ρ_B , the maximum amount of hydrogen that can be stored in the pore, m_A^{\max} , and a Type I isotherm equation for fractional filling, Θ_A , as a function of pressure and temperature. Note that the factor of 100 is included in Equation (1) in order to balance units, as all excess isotherms used have been converted to weight percent (wt%) relative to the dry activated (degassed) sample weight.

$$m_E = m_A^{\max} \Theta_A - 100 \rho_B v_P \quad (1)$$

There are many different Type I isotherm equations in the literature, both fundamental and empirical, many of which account for factors such as surface energy and pore size distributions (Do 1998; Jaroniec, Madey 1988; Rouquerol et al. 1998; Rudzinski, Everett 1992).

One of the earliest recognised isotherm equations was derived by Irving Langmuir in 1918, (Equation 2), and is aptly named the Langmuir equation. It is an equation that calculates the coverage of adsorbed molecules on a surface with respect to pressure, at a fixed temperature (Langmuir 1918) and assumes an energetically homogenous surface.

$$\Theta_A = \frac{bP}{1 + bP} \quad (2)$$

where P is the absolute pressure of the system, and b is the affinity parameter, a constant relating to the strength of adsorption onto the surface, which is usually assumed to follow an Arrhenius relationship (Arrhenius 1889):

$$b = b_0 \exp\left(\frac{Q}{RT}\right) \quad (3)$$

where Q is related to the enthalpy of adsorption, b_0 is the pre-exponential factor and relates to the entropy of adsorption, R is the molar gas constant and T is the absolute temperature.

The simple Langmuir model has been extended to account for heterogeneous surfaces. Some well-known examples of these developments include the Tóth equation (Toth 1962) and the Freundlich equation (Freundlich 1926) both of which have been used for hydrogen adsorption analysis by Gil et al. (2009), the Sips equation (Sips 1948) which has been used for analysis by Johansson et al. (2002), the modified Dubinin-Astakhov equation (Richard et al. 2009) which has been used for analysis by Poirier et al. (2006), and the Langmuir-Freundlich equation which has been used for analysis by Choi et al. (2003).

In order to explore the application and credibility of these and other adsorption models for extraction of a variety of parameters including the total hydrogen uptake, selected isotherm equations were applied to hydrogen uptake data for six different nanoporous materials as detailed in the following sections.

2. Experimental section

2.1 Materials and characterisation

TE7 carbon beads are a well characterised reference material, sourced from MAST Carbon International, Basingstoke, UK. They have a Brunauer, Emmett and Teller (BET) nitrogen specific surface area of $960 \pm 50 \text{ m}^2 \text{ g}^{-1}$ (where the uncertainty here and elsewhere in this section refers to the standard deviation), obtained using the British Standard Method (British Standards Institution 1996) from low pressure nitrogen sorption measurements on a Micromeritics ASAP

1 2020 volumetric adsorption analyser at 77 K with a 60 minute equilibration time
2 (Hruzewicz-Kołodziejczyk et al. 2012). This material has a micropore volume of
3 $0.43 \pm 0.03 \text{ cm}^3 \text{ g}^{-1}$, evaluated from the Dubinin-Radushkevich method (Dubinin
4 1975), and a skeletal volume of $1.90 \pm 0.03 \text{ g cm}^{-3}$, measured using a He
5 pycnometer (Micromeritics AccuPyc 1330). Samples were degassed for 8 hours at
6 623 K prior to measurement of high pressure hydrogen sorption isotherms at 77
7 K, 89 K, 102 K, 120 K and 150 K up to a maximum pressure of 14 MPa, using a
8 Hiden HTP-1 Sieverts-type volumetric gas sorption analyser.

9
10 AX-21 activated carbon was sourced from Anderson Development Company Inc.,
11 Michigan, United States. This material has a BET nitrogen specific surface area of
12 $2448 \pm 40 \text{ m}^2 \text{ g}^{-1}$, and a relatively broad pore size distribution compared to the
13 TE7 carbon beads, with the majority of pores being around 1.4 nm, but with
14 approximately 20 % of pores in the mesopore region (between 2 and 50 nm)
15 (Zhou et al. 2000) . Samples were degassed for 12 hours at 473 K prior to
16 measurement of high pressure hydrogen sorption isotherms at 90 K, 100 K, 110 K
17 and 120 K up to a maximum pressure of 18 MPa, using a Hiden HTP-1 Sieverts-
18 type volumetric gas sorption analyser.

19
20 The chromium (III) terephthalate metal-organic framework
21 $[\text{Cr}_3\text{O}(\text{bdc})_3(\text{OH},\text{F})(\text{H}_2\text{O})_2]$, MIL-101(Cr), (where MIL stands for ‘Matériaux de
22 l’Institut Lavoisier’, and bdc is benzene-1,4-dicarboxylate) was prepared by
23 adapting the method reported previously by Jiang et al. (2011). 0.33 g of
24 terephthalic acid $[\text{C}_6\text{H}_4\text{-1,4-(CO}_2\text{H)}_2]$ was added to 0.8 g chromium (III) nitrate
25 nonahydrate $[\text{Cr}(\text{NO}_3)_3 \cdot 9\text{H}_2\text{O}]$ in a Teflon-lined autoclave, with 10 mL distilled
26 water and a stirrer bar. This was heated to 453 K and left for 8 hours, before
27 cooling overnight to room temperature. The white powder formed was washed
28 with deionised water and vacuum filtered to form a blue/green suspension, which
29 was centrifuged three times in water for 10 minutes each time at 11000 rpm and
30 left to dry, resulting in a green solid. Following the synthesis, the solvent was
31 removed from the pores by drying in a vacuum oven, and then degassing at 423 K
32 for 4 hours. MIL-101(Cr) is a rigid, well-studied MOF with pore sizes ranging
33 between 2.9-3.4 nm (Férey et al. 2005), and a BET nitrogen surface area of 2887
34 $\pm 106 \text{ m}^2 \text{ g}^{-1}$. Samples were degassed for 4 hours at 423 K prior to measurement

1 of high pressure hydrogen sorption isotherms at 77 K, 90 K, 100 K and 110 K up
2 to a maximum pressure of 18 MPa, using a Hiden HTP-1 Sieverts-type volumetric
3 gas sorption analyser.

4

5 [Al(OH)(bdc)], MIL-53(Al), was prepared by adapting the previously reported
6 synthetic procedure (Loiseau et al. 2004). 0.165 g of terephthalic acid [C₆H₄-1,4-
7 (CO₂H)₂] was added to 0.376 g aluminium (III) nitrate nonahydrate
8 [Al(NO₃)₃·9H₂O] in a Teflon-lined autoclave, with 10 mL distilled water and a
9 stirrer bar. This was heated to 493 K and left for 8 hours, before cooling overnight
10 to room temperature. The white powder formed was then washed with acetone
11 and vacuum filtered to form a clear liquid, which was centrifuged three times in
12 acetone for 10 minutes each time at 11000 rpm and left to dry, resulting in a white
13 solid. The solvent was then removed from the pores by drying in a vacuum oven,
14 and then degassing at 423 K for 4 hours. This material was chosen due to its
15 propensity for breathing or pore distortion (Boutin et al. 2009; Serre et al. 2007;
16 Neimark et al. 2011). This behavior is thought to occur with changes in either
17 temperature, pressure, or introduction of a guest molecule, which causes the pores
18 to stretch, reducing the volume within. The pore sizes in MIL-53(Al) vary
19 between 1.7 – 2.1 nm, and 1.3 – 0.7 nm, between the large pore and narrow pore
20 structures respectively (Liu et al. 2008), and the material has a BET nitrogen
21 surface area of $1118 \pm 47 \text{ m}^2 \text{ g}^{-1}$. Samples were degassed for 4 hours at 423 K
22 prior to measurement of high pressure hydrogen sorption isotherms at 77 K, 90 K,
23 100 K, 110 K and 120 K up to a maximum pressure of 18 MPa, using a Hiden
24 HTP-1 Sieverts-type volumetric gas sorption analyser.

25

26 NOTT-101 is a copper-based MOF, with the formula Cu₂(tp^{tc}) (where tp^{tc} is
27 terphenyl-3,3'',5,5''-tetracarboxylate), and was originally synthesised in
28 Nottingham in 2006 (Lin et al. 2006). It has an average pore size of 0.65 nm, and
29 a BET surface area of $2510 \text{ m}^2 \text{ g}^{-1}$. The hydrogen sorption data was provided by
30 Anne Dailly from General Motors Research and Development Centre (GM
31 Research and Development Centre, Warren, MI, USA) from hydrogen isotherm
32 measurements at 50 K, 60 K, 70 K, 77 K and 87 K (Poirier, Dailly 2009).

33

1 Zeolitic imidazolate framework 8 (ZIF-8) is a MOF that is topologically
2 isomorphic with a sodalite (SOD) zeolite . It consists of a tetrahedrally-
3 coordinated zinc centre linked by imidazolate, and the pores are 1.16 nm in
4 diameter, connected by small apertures of 0.34 nm. ZIF-8 was first reported in
5 2006 (Park et al. 2006), and the hydrogen sorption isotherms were obtained from
6 the literature using EnGauge data-reading software at 50 K, 60 K, 77 K, 100 K
7 and 125 K (Zhou et al. 2007).

8 **2.2 High pressure hydrogen sorption measurements**

9 High pressure volumetric gas sorption studies were conducted on a Hiden HTP-1
10 Sieverts-type volumetric gas sorption analyser up to pressures of 20 MPa. High
11 purity hydrogen was used for all of the measurements (99.99996 %, BIP-Plus
12 from Air Products), with the 77 K isotherms using a liquid nitrogen bath for
13 temperature control. Prior to each measurement, the samples (typically 100 mg)
14 were degassed in order to remove impurities from surfaces and pores, applying a
15 minimum equilibration time of 12 minutes. All isotherms presented in this paper
16 measured using the HTP-1 were fully reversible, and repeat isotherms were
17 reproduced to within 0.3 % of the measured amounts adsorbed. All isotherms are
18 reported as excess hydrogen uptake in wt% relative to the degassed sample
19 weight.

20 **2.3 Data Analysis**

21 All non-linear fitting was carried out using the Origin 8.5 Pro software (OriginLab
22 Corporation, Massachusetts, United States). This programme uses a Levenberg-
23 Marquardt method of non-linear fitting (Marquardt 1963), which combines the
24 steepest-descent method and the Gauss-Newton method to adjust the parameter
25 values to achieve the minimum χ^2_{red} value (a measure of the quality of fit). Up to
26 400 fitting iterations were carried out with a tolerance of 10^{-9} .

27 **3. Mathematical model**

28 An improvement on the general model (Equation 1) is described, taking into
29 account density variation of fluid within pores. This allows for an adsorbate
30 (adsorbed phase) with a higher density, ρ_A , than that of the bulk gas, ρ_B (Fig. 1).
31 The sections of the graph of the density profile of the hydrogen in the pore (Fig.

1) containing vertical lines represents m_E . The sections containing the vertical lines plus the sections containing the diagonal lines (where the section containing the diagonal lines indicates the amount of hydrogen that would be within the area of the adsorbate if there were no interactions with the surface, $m_{B(A)}$) represents the absolute amount of hydrogen, which is the total amount of hydrogen within the adsorbate, m_A . The sections containing the vertical lines, plus the sections containing the diagonal lines, plus the section containing the horizontal dashed lines (where the section containing the horizontal dashed lines indicates the amount of bulk hydrogen) represents the total amount of hydrogen within the pores, m_P (Schlichtenmayer, Hirscher 2012).

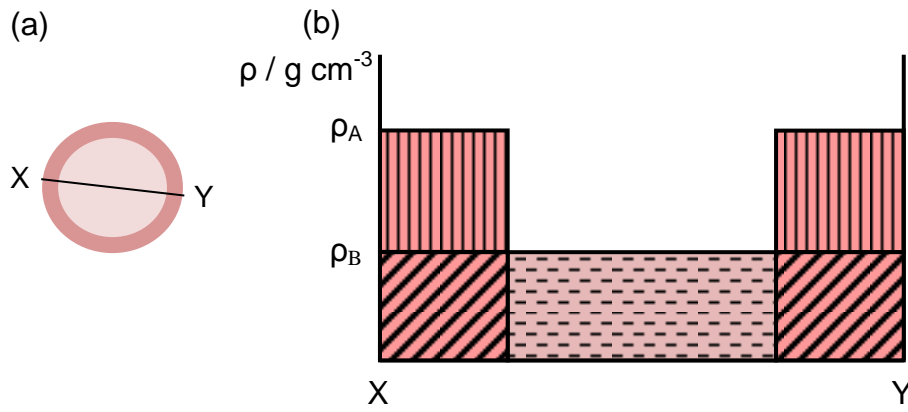


Fig. 1 Assumed hydrogen density profile within a pore. (a) A cross-sectional diagram of the pore. (b) The corresponding density profile, with the x axis representing the cross section of the pore, where ρ_A represents the mass density of the adsorbate, and ρ_B represents the mass density of the bulk hydrogen

3.1 Derivation of the model

As the excess hydrogen is equal to the total amount of hydrogen within the adsorbate minus the bulk amount of hydrogen within the adsorbate, it can be stated that

$$m_E = m_A - m_{B(A)} \quad (4)$$

where

$$m_A = \rho_A v_A \quad (5)$$

where ρ_A is the density of the adsorbate, and v_A is the volume of the adsorbate, and

$$m_{B(A)} = \rho_B v_A \quad (6)$$

Therefore, substituting Equations (5) and (6) into Equation (4) gives

$$m_E = \rho_A v_A - \rho_B v_A \quad (7)$$

which can be simplified to give

$$m_E = (\rho_A - \rho_B) v_A \quad (8)$$

Note that the total amount in the pore is

$$m_P = m_E + \rho_B v_P \quad (9)$$

The bulk adsorptive density can be determined using an equation of state

$$\rho_B = \frac{1}{Z} \frac{PM}{RT} \quad (10)$$

where M is molar mass and Z is the compressibility factor (for an ideal gas, $P \rightarrow 0$, $Z \rightarrow 1$). We use a rational approximation (Bimbo et al. 2011) to the Leachman equation of state for hydrogen (Leachman et al. 2009), which is available through the National Institute of Standards and Technology (NIST) website (National Institute of Standards and Technology 2011).

A fractional filling term, Θ_A , is defined as,

$$\Theta_A = \frac{v_A}{v_P} \quad (11)$$

We assume Θ_A is of the form of an IUPAC Type I isotherm. Therefore, substituting Equations (10) and (11) into Equation (8), the following equation has been derived

$$m_E = \left(\rho_A - \frac{1}{Z} \frac{PM}{RT} \right) 100 v_P \Theta_A \quad (12)$$

The multiplier of 100 has been included into the equation in order to balance units, as described above. Equation (12) is the model framework for analysing experimental excess adsorption isotherms.

3.2 A direct comparison between the two equations

A comparison between the average density model (Equation 1) and the model incorporating a density variation (Equation 12) has been made, shown here using the TE7 carbon beads and the Tóth isotherm equation (Equation 13) as an example:

$$\Theta_A = \frac{b_{(T)}P}{\left(1 + (b_{(T)}P)^{c_{(T)}}\right)^{\frac{1}{c_{(T)}}}} \quad (13)$$

where $b_{(T)}$ is the Tóth affinity parameter and $c_{(T)}$ is the Tóth heterogeneity parameter.

The root mean square residual (RMSR), explained in the Online Resource, has been used as a method of comparing the quality of the fits, with lower values indicating a better quality of fit (Fig. 2):

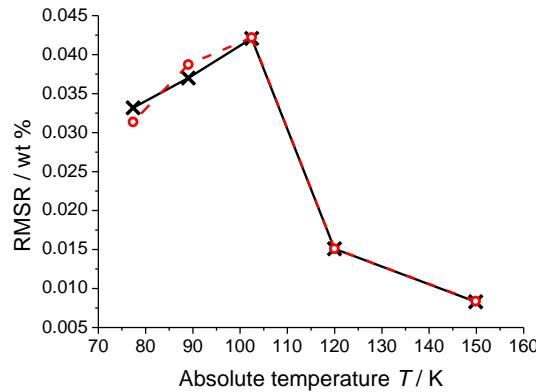


Fig. 2 A comparison of the average density model and the model incorporating a density variation, using the Tóth equation, and fit to isotherms from the TE7 carbon beads. Straight lines were used to join the points to guide the eye, with the dotted line linking the open circles of the model incorporating the density variation (Equation 12), and the solid line linking the crosses of the average density model (Equation 1)

Bias was also examined for both of the sets of fits, as well as the use of other isotherm equations as described in the Online Resource. While both models fit the data with very similar RMSR values, the improved model was chosen for detailed study as it explicitly accounts for adsorbate density.

3.3 Derivation of the Unilan- b equation

In order to extend and further test the analysis a new isotherm equation was described, the Unilan- b (Equation 14). This new equation is similar to the more familiar Unilan- Q equation (Equation 15) (Honig,Reyerson 1952), but assumes a different heterogeneity function.

$$\Theta_A = 1 - \frac{1}{P(b_2 - b_1)} \ln \left(\frac{1 + b_2 P}{1 + b_1 P} \right) \quad (14)$$

$$\Theta_A = \frac{RT}{Q_2 - Q_1} \ln \left(\frac{1 + b_0 \exp \left(\frac{Q_2}{RT} \right) P}{1 + b_0 \exp \left(\frac{Q_1}{RT} \right) P} \right) \quad (15)$$

where b_1 and b_2 are the minimum and maximum values of the affinity parameter b respectively and Q_1 and Q_2 are the minimum and maximum values of the energy parameter Q respectively.

The Unilan- Q equation uses a uniform distribution function with respect to Q , whereas the Unilan- b equation uses a uniform distribution with respect to b (Fig. 3), with the two parameters being related according to Equation (3). The derivation of the Unilan- b equation can be observed in the Online Resource.

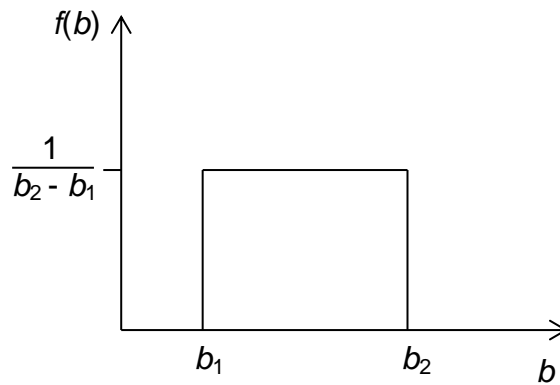


Fig. 3 The distribution of the affinity parameter for the Unilan- b equation. b is in inverse units of pressure, and $f(b)$ is in units of pressure

The Unilan- b equation follows Henry's Law in the limit of low pressure, saturates to unity at high pressure, and reduces to the Langmuir equation when b_2 approaches b_1 (in which case $f(b)$ approaches the Dirac delta function).

1
2 There are notable benefits arising from the new Unilan- b equation compared with
3 the original Unilan- Q equation. Firstly, b is considered as the single adjustable
4 parameter since A and Q in the Arrhenius equation may be correlated via the
5 ‘compensation effect’ (Wilson, Galwey 1973). Secondly, the Unilan- b equation is
6 far simpler to implement and has fewer parameters than the Unilan- Q equation.
7 The most preferable equation to use for the comparison of different materials for
8 hydrogen uptake would be one that fits the data, but with the fewest number of
9 parameters. This follows Occam’s razor, which states that when choosing between
10 models, the one with the fewest assumptions is preferred.

11 **4. Results and discussion**

12 **4.1 Selection of variables**

13 Equation (12) was used as the model for analysis of the experimental excess
14 hydrogen adsorption data for the six different nanoporous materials described in
15 Section 2.1. Initially, constant adsorbate density ρ_A and pore volume v_p were
16 assumed, and eight different Type I isotherms were tested for Θ_A . The materials
17 were chosen to include a range of different types of materials with different pore
18 sizes and volumes, some of which were synthesised and analysed in Bath, some of
19 which were sourced externally and then analysed in-house, and some of which the
20 information was collected from published literature. A wide range of isotherms
21 that have previously been used to model hydrogen adsorption in literature were
22 chosen, in order to examine the greatest variations between the models. The
23 majority of these equations are well known Type I equations, each embedding a
24 range of characteristic parameters. The eight different isotherm equations used are
25 summarised in Table 1.

26
27 **Table 1** A summary of the Type I isotherm equations used within the study

Name (Reference)	Equation and explanation of terms	Number of parameters
Langmuir (Langmuir 1918)	$\Theta_A = \frac{b_{(L)}P}{1 + b_{(L)}P} \quad (2)$	1

$b_{(L)}$ is the Langmuir affinity parameter			
Tóth (Toth 1962)	$\Theta_A = \frac{b_{(T)}P}{\left(1 + (b_{(T)}P)^{c_{(T)}}\right)^{\frac{1}{c_{(T)}}}} \quad (13)$		2
Sips (Sips 1948)	$\Theta_A = \frac{(b_{(S)}P)^{\frac{1}{m_{(S)}}}}{1 + (b_{(S)}P)^{\frac{1}{m_{(S)}}}} \quad (16)$		2
$b_{(S)}$ is the Sips affinity parameter			
$m_{(S)}$ is the Sips heterogeneity parameter			
Generalised Freundlich (Sips 1950)	$\Theta_A = \left(\frac{b_{(GF)}P}{1 + b_{(GF)}P}\right)^q \quad (17)$		
	$b_{(GF)}$ is the Generalised Freundlich affinity parameter		2
	q is the Generalised Freundlich heterogeneity parameter		
Jovanović- Freundlich (Quiñones,Guiochon 1996)	$\Theta_A = 1 - \exp(-(b_{(JF)}P)^{c_{(JF)}}) \quad (18)$		
	$b_{(JF)}$ is the Jovanović-Freundlich affinity parameter		2
	$c_{(JF)}$ is the Jovanović-Freundlich heterogeneity parameter		
	$\Theta_A = \exp\left(\frac{RT}{\alpha + \beta T}\right)^{m_{(DA)}} \ln\left(\frac{P_0}{P}\right)^{m_{(DA)}} \quad (19)$		
	α is the Dubinin-Astakhov enthalpic factor		
Dubinin-Astakhov (Richard et al. 2009)	β is the Dubinin-Astakhov entropic factor		4
	$m_{(DA)}$ is an adjustable parameter in the Dubinin-Astakhov equation		
	P_0 is the vapour pressure (non-existent for a supercritical fluid, therefore a parameter from the fit)		

Unilan- Q (Honig,Reyerson 1952)	$\Theta_A = \frac{RT}{Q_2 - Q_1} \ln \left(\frac{1 + b_0 \exp\left(\frac{Q_2}{RT}\right) P}{1 + b_0 \exp\left(\frac{Q_1}{RT}\right) P} \right) \quad (15)$	3
Unilan- b (this work)	$\Theta_A = 1 - \frac{1}{P(b_2 - b_1)} \ln \left(\frac{1 + b_2 P}{1 + b_1 P} \right) \quad (14)$	2

1

2 **4.2 Fitting methodology**

3 The first step in the analysis involved fitting Equation (12) for a selected Type I
4 filling function Θ_A to each individual isotherm for all of the materials separately,
5 constituting a total of 216 fits. Estimated values of v_p and ρ_A and of parameters of
6 the Type I isotherm equation for a given material were then plotted as a function
7 of temperature. These plots indicated that neither pore volume nor the adsorbate
8 density depended on temperature and were therefore assumed to be constants for a
9 given Type I isotherm and material. It should be noted that implicit in all these fits
10 was an assumption that none of the parameters were dependent upon pressure. In
11 future work the possible pressure dependence of v_p and ρ_A will be explored in
12 more detail.

13

14 Global fits (fits over the entire temperature range for each material assuming v_p
15 and ρ_A to be constant, but allowing each parameter within the Type I isotherm
16 equations to vary) were then conducted on the variable temperature hydrogen
17 sorption datasets for each material for each Type I isotherm equation within the
18 model. These global fits are deposited in the Online Resource, except for the fits
19 using the Tóth isotherm equation, which are illustrated in Fig. 4. Table 2 shows
20 the parameter values for the global fit of the Tóth isotherm equation to the H_2
21 adsorption data for the TE7 carbon beads, which is the most well-characterised
22 material of the six materials examined. Parameter values for the Tóth global fits
23 for the remaining five materials are in the Online Resource for comparison.

24

25

26

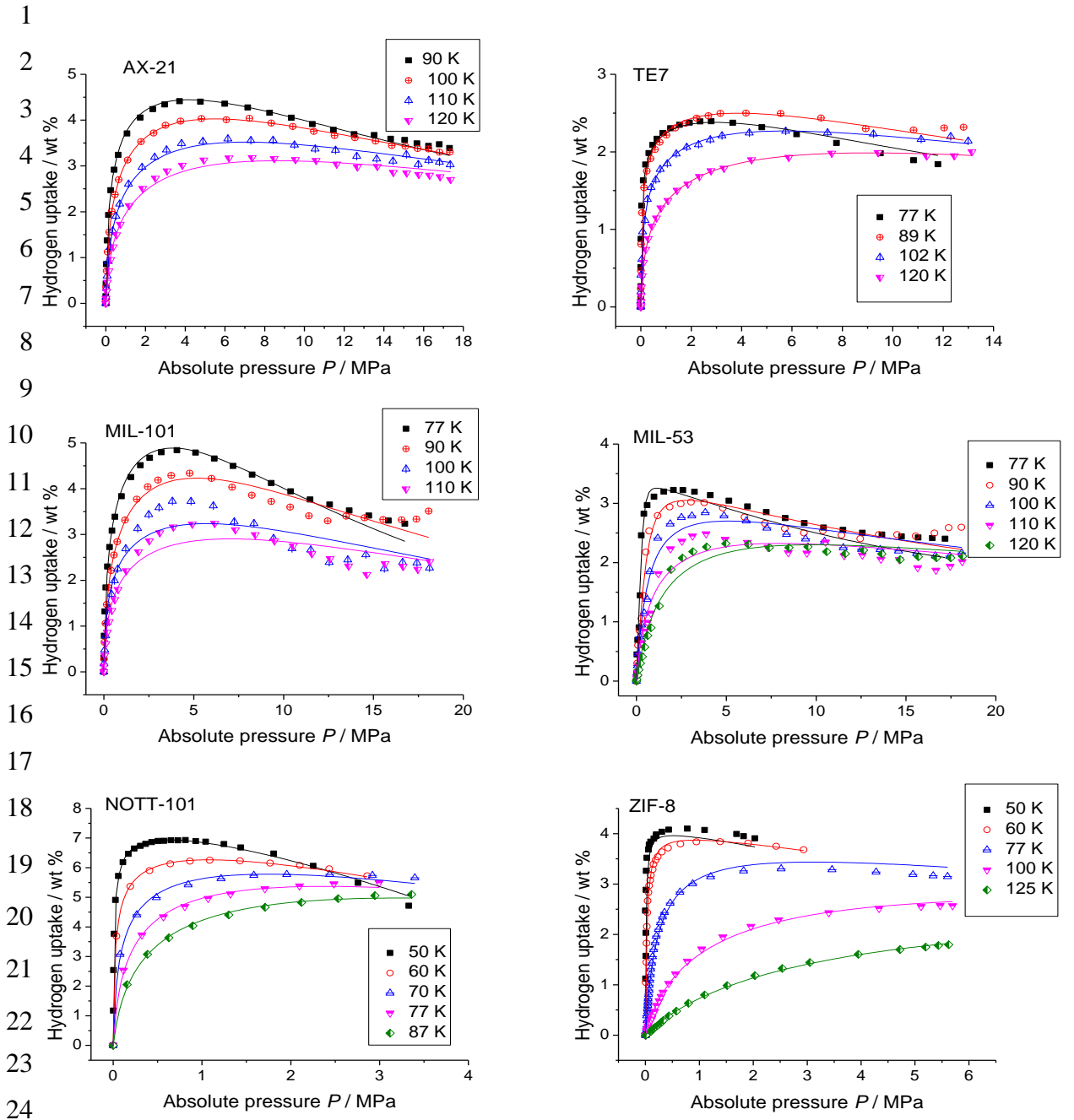
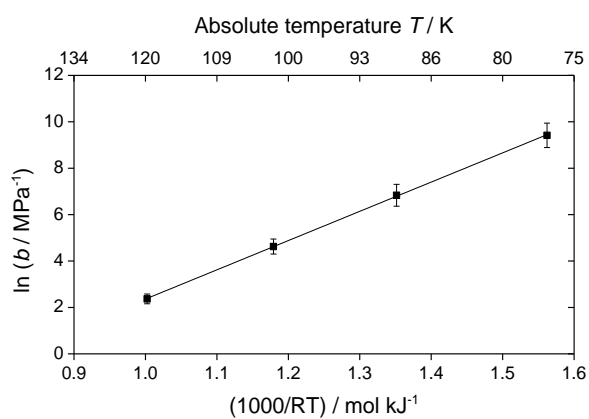


Fig. 4 Global fits using the Tóth equation to all of the materials. The points indicate the experimental data, with the lines showing the fits. The colour of the lines indicating the fits match the colour coding of the temperatures in the figure legend

1 **Table 2** Parameter values estimated from the global fits using the Tóth model for H₂ isotherms on
2 the TE7 carbon beads. Uncertainties are standard errors

Temperature / K	$b_{(T)} /$ MPa ⁻¹	$c_{(T)} /$ -	$v_P /$ cm ³ g ⁻¹	$\rho_A /$ g cm ⁻³
77	12300 ± 6460	0.200 ± 0.0140	0.469 ± 0.0544	0.100 ± 0.00448
89	927 ± 437	0.245 ± 0.0197		
102	102 ± 33.2	0.275 ± 0.0197		
120	10.7 ± 2.25	0.316 ± 0.0198		

3



4

5 **Fig. 5** An Arrhenius plot for b for the Tóth fit to the TE7 carbon beads. The line of best fit is
6 created using a linear least squares method. The error bars are standard errors

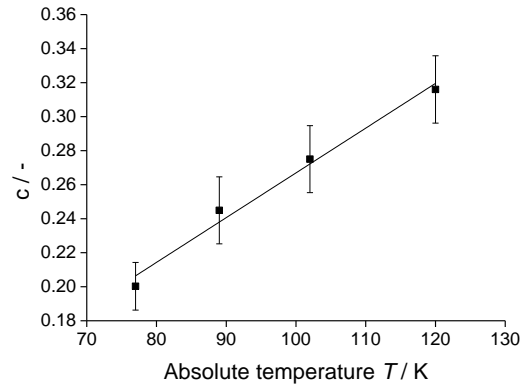


Fig. 6 Values of c with temperature refined from the fit using the Tóth model on the isotherms of the TE7 carbon beads. The line of best fit is created using a linear least squares method. The error bars are standard errors

Fig. 5 shows that the Tóth affinity parameter $b_{(T)}$ depends on T according to an Arrhenius relationship, as expected from Equation (3). The c parameter appears to increase with increasing T (Fig. 6). This is not unexpected as the effects of heterogeneity reduce with increasing T (in the limit $c \rightarrow 1$, the heterogeneous Tóth isotherm approaches the homogeneous Langmuir isotherm), and the value of v_P is very close to the pore volume of $0.43 \text{ cm}^3 \text{ g}^{-1}$ obtained from the N_2 isotherm at 77 K using the Dubinin-Radushkevich method. Remarkably, ρ_A is estimated to be about 0.1 g cm^{-3} , indicating a solid-like density of hydrogen within the pores (Silvera 1980). The presence of solid-like H_2 in nanopores has been predicted previously using Grand-Canonical Monte Carlo (GCMC) simulations (Jagiello et al. 2006; Wang,Johnson 1998). Overall, the Tóth model produced realistic values and trends for all of the parameters when used to fit to H_2 adsorption data for the TE7 carbon beads in the temperature and pressure ranges examined.

4.3 Comparison of the quality of fit between Type I isotherms

The RMSR was used as a measure of the quality of fit for each of the eight isotherm models for each of the six adsorbents. Fig. 7 shows cumulative RMSR data for each model, and Fig. 8 shows individual RMSR data for each model of the six materials.

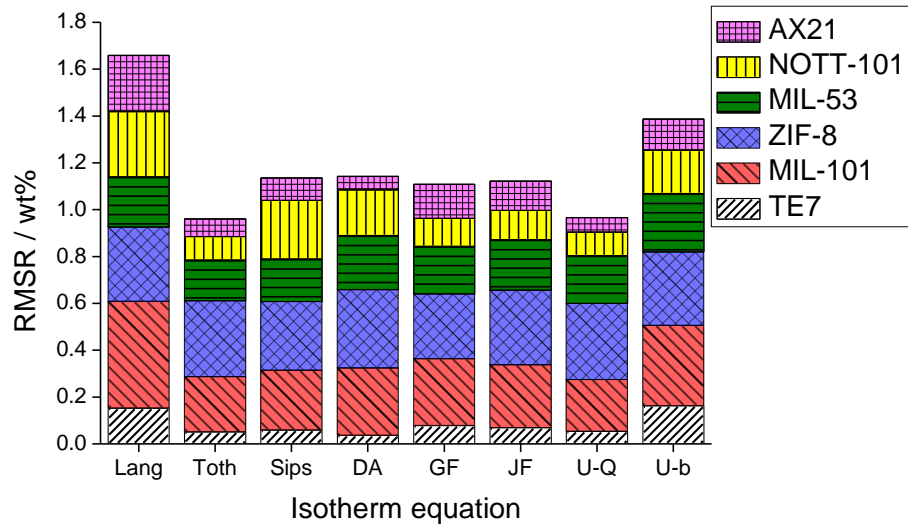


Fig. 7 Cumulative RMSR for each isotherm equation

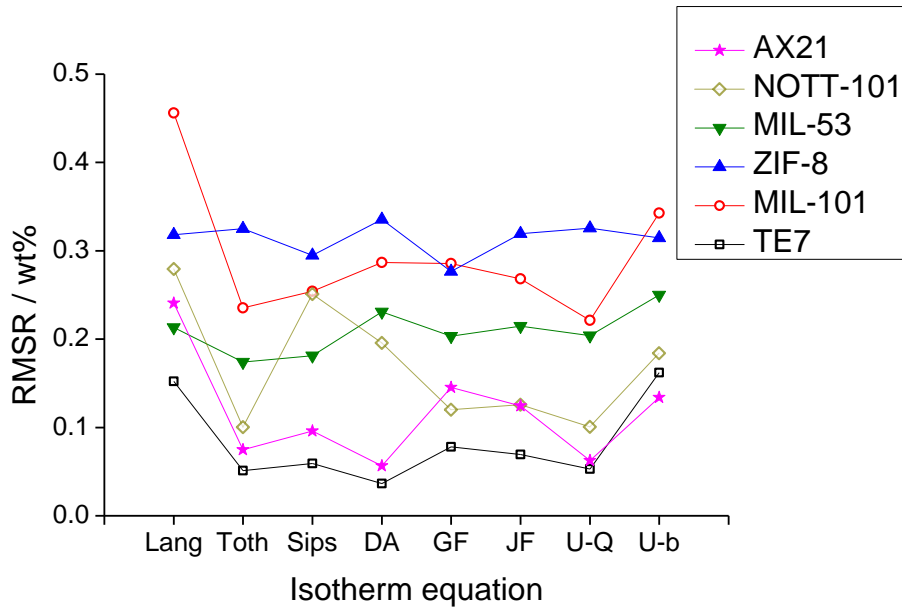


Fig. 8 RMSR for each isotherm equation and each material. Straight lines are drawn between points to guide the eye

Both Fig. 7 and Fig. 8 show the same information, represented in different ways in order to emphasise different features. Fig. 7 shows that overall, the Langmuir and the Unilan-*b* equations have the worst fits to the data in terms of RMSR, and the Tóth and the Unilan-*Q* have the best fits to the data, with the other four equations having relatively similar quality of fits.

1 However, Fig. 8 shows that even though the Tóth has the best fit overall to the
2 data, it is not the best equation to use for every material. For example, the Sips
3 equation and the Generalized Freundlich equation both have better fits to the ZIF-
4 8 data than the Tóth equation. It also shows that generally, all of the equations fit
5 better to the carbon materials (TE7 and AX-21) than the MOFs, and the worst fits
6 are to the ZIF data. This result could be affected by the capacity of the materials,
7 as higher capacities could result in higher RMSR values. Another point to note
8 from Fig. 8 is that some equations show much higher RMSRs for certain materials
9 than expected. For example, the Sips and the Dubinin-Astakhov equations show
10 much higher RMSRs for NOTT-101 in comparison to the other equations than
11 they do for other materials.

12 **5. Conclusions**

13 A new model that incorporates a more realistic description of fluid density inside
14 pores has been derived and results in fits to experimental excess adsorption
15 isotherm data to a very similar standard as the former average density model, but
16 is able to distinguish between the amounts of hydrogen adsorbate and bulk
17 hydrogen within pores. This new description (Equation 12) could prove useful not
18 only for the analysis of supercritical hydrogen sorption data, but could also be
19 applied to data from other supercritical adsorptives such as methane and carbon
20 dioxide. The remarkable observation of solid-like densities for hydrogen
21 adsorbate in a TE7 carbon bead material suggests future positive options for
22 hydrogen storage in similar materials to meet demanding targets set, for example,
23 by the U.S. Department of Energy (U.S. Department of Energy 2009).

24
25 Statistical comparison of different Type I isotherm models for the pore filling
26 function, Θ_A , in the new model suggests that the Tóth equation (one
27 heterogeneous version of the Langmuir equation) may, on average, be the best
28 choice in terms of quality of fit for hydrogen adsorption isotherms over a range of
29 nanoporous materials. However, this is not a universal trend; for example the
30 relatively simple new Unilan- b equation appears to be a good model for
31 adsorption on the ZIF-8 material, and the reasons why different isotherms produce
32 different results may well be due to differences in quantities such as pore shapes
33 and sizes, rigidity of the materials, total adsorption capacities and the assumptions

built into the different isotherm equations. One aspect that will be studied in more detail using the new model, which will be reported in due course, is the pressure and temperature dependence of adsorbate density and pore volume.

Acknowledgements

JES thanks the UK Engineering and Physical Sciences Research Council (EPSRC) Doctoral Training Centre in Sustainable Chemical Technologies at the University of Bath, and also to Dr Agata Godula-Jopek from the EADS Innovation Works, Munich, Germany for financial support. NB and TJM thank the EPSRC for funding via the SUPERGEN United Kingdom Sustainable Hydrogen Energy Consortium (UK-SHEC, EP/J016454/1), VPT thanks the University of Bath for funding via an EPSRC Development Fund grant and a Prize Research Fellowship, and VPT and TJM thank the EPSRC for supporting the latter stages of this work via its Delivery Fund at the University of Bath and the SUPERGEN Hydrogen and Fuel Cells Hub (EP/E040071/1). JES, NB and VPT thank the Organising Committee of the 8th International Symposium of the Effects of Surface Heterogeneity in Adsorption and Catalysis on Solids (ISSHAC-8, Aug 2012, Krakow, Poland) for the opportunity to present this work as an oral presentation and for subsidising registration for the conference. ADB and DJ thank the EPSRC for funding (EP/H046305/1).

References:

- Arrhenius, S.: *Über die Reaktionsgeschwindigkeit bei der Inversion von Rohrzucker durch Säuren*. Z. Physik. Chem. **4**, 226 (1889)
- Bekkum, H.V.: *Introduction to Zeolite Science and Practice*. vol. 137. Elsevier, (2001)
- Bimbo, N., Ting, V.P., Hruzewicz-Kolodziejczyk, A., Mays, T.J.: Analysis of hydrogen storage in nanoporous materials for low carbon energy applications. *Faraday Discuss.* **151**(0), 59-74 (2011)
- Boutin, A., Springuel-Huet, M.-A., Nossov, A., Gédéon, A., Loiseau, T., Volkringer, C., Férey, G., Coudert, F.-X., Fuchs, A.H.: Breathing Transitions in MIL-53(Al) Metal–Organic Framework Upon Xenon Adsorption. *Angew. Chem. Int. Edit.* **48**(44), 8314-8317 (2009)
- British Standards Institution: Determination of the specific surface area of powders-part 1: BET method of gas adsorption for solids (including porous materials). In. [BS 4359-1, ISO 9277:1995] British Standards Institution, (1996)
- Choi, B.-U., Choi, D.-K., Lee, Y.-W., Lee, B.-K., Kim, S.-H.: Adsorption Equilibria of Methane, Ethane, Ethylene, Nitrogen, and Hydrogen onto Activated Carbon. *J. Chem. Eng. Data* **48**(3), 603-607 (2003)
- Czerny, A.M., Bénard, P., Chahine, R.: Adsorption of Nitrogen on Granular Activated Carbon: Experiment and Modeling. *Langmuir* **21**(7), 2871-2875 (2005)
- Do, D.D.: *Adsorption Analysis: Equilibria and Kinetics*, vol. 2. Series on Chemical Engineering. Imperial College Press, (1998)
- Dubinin, M.M.: *Progress in Surface and Membrane Science*. In: Cadenhead, D.A. (ed.). vol. 9. Academic Press, New York (1975)

- 1 Férey, G., Mellot-Draznieks, C., Serre, C., Millange, F., Dutour, J., Surblé, S.,
2 Margiolaki, I.: A Chromium Terephthalate-Based Solid with Unusually
3 Large Pore Volumes and Surface Area. *Science* **309**(5743), 2040-2042
4 (2005)
- 5 Freundlich, H.: *Colloid & Capillary Chemistry*. Methuen & Co. Ltd., (1926)
- 6 Gil, A., Trujillano, R., Vicente, M.A., Korili, S.A.: Hydrogen adsorption by
7 microporous materials based on alumina-pillared clays. *Int. J. Hydrogen*
8 *Energ.* **34**(20), 8611-8615 (2009)
- 9 Honig, J.M., Reyerson, L.H.: Adsorption of Nitrogen, Oxygen and Argon on
10 Rutile at Low Temperatures; Applicability of the Concept of Surface
11 Heterogeneity. *J. Phys. Chem.* **56**(1), 140-144 (1952)
- 12 Hruzewicz-Kołodziejczyk, A., Ting, V.P., Bimbo, N., Mays, T.J.: Improving
13 comparability of hydrogen storage capacities of nanoporous materials. *Int.*
14 *J. Hydrogen Energ.* **37**(3), 2728-2736 (2012)
- 15 Jagiello, J., Ansón, A., Martínez, M.T.: DFT-Based Prediction of High-Pressure
16 H₂ Adsorption on Porous Carbons at Ambient Temperatures from Low-
17 Pressure Adsorption Data Measured at 77 K. *J. Phys. Chem. B* **110**(10),
18 4531-4534 (2006)
- 19 James, S.L.: Metal-organic frameworks. *Chem. Soc. Rev.* **32**(5), 276-288 (2003)
- 20 Jaroniec, M., Madey, R.: *Physical adsorption on heterogeneous solids*. Elsevier,
21 (1988)
- 22 Jiang, D., Burrows, A.D., Edler, K.J.: Size-controlled synthesis of MIL-101(Cr)
23 nanoparticles with enhanced selectivity for CO₂ over N₂. *Cryst. Eng.*
24 *Comm.* **13**(23), 6916-6919 (2011)
- 25 Johansson, E., Hjärvansson, B., Ekström, T., Jacob, M.: Hydrogen in carbon
26 nanostructures. *J. Alloy Compd.* **330–332**(0), 670-675 (2002)
- 27 Langmuir, I.: The Adsorption of Gases on Plane Surfaces of Glass, Mica and
28 Platinum. *J. Am. Chem. Soc.* **40**(9), 1361-1403 (1918)
- 29 Leachman, J.W., Jacobsen, R.T., Penoncello, S.G., Lemmon, E.W.: Fundamental
30 Equations of State for Parahydrogen, Normal Hydrogen, and
31 Orthohydrogen *J. Phys. Chem. Ref. Data* **38**(721) (2009)
- 32 Lin, X., Jia, J., Zhao, X., Thomas, K.M., Blake, A.J., Walker, G.S., Champness,
33 N.R., Hubberstey, P., Schröder, M.: High H₂ Adsorption by Coordination-
34 Framework Materials. *Angew. Chem. Int. Edit.* **45**(44), 7358-7364 (2006)
- 35 Liu, Y., Her, J.-H., Dailly, A., Ramirez-Cuesta, A.J., Neumann, D.A., Brown,
36 C.M.: Reversible Structural Transition in MIL-53 with Large Temperature
37 Hysteresis. *J. Am. Chem. Soc.* **130**(35), 11813-11818 (2008)
- 38 Loiseau, T., Serre, C., Huguenard, C., Fink, G., Taulelle, F., Henry, M., Bataille,
39 T., Férey, G.: A Rationale for the Large Breathing of the Porous
40 Aluminum Terephthalate (MIL-53) Upon Hydration. *Chem. Eur. J.* **10**(6),
41 1373-1382 (2004)
- 42 Marquardt, D.W.: An Algorithm for Least-Squares Estimation of Nonlinear
43 Parameters. *J. Soc. Ind. Appl. Math.* **11**(2), 431-441 (1963)
- 44 McKeown, N.B., Budd, P.M.: Polymers of intrinsic microporosity (PIMs):
45 organic materials for membrane separations, heterogeneous catalysis and
46 hydrogen storage. *Chem. Soc. Rev.* **35**(8), 675-683 (2006)
- 47 National Institute of Standards and Technology: NIST Chemistry WebBook.
48 <http://webbook.nist.gov/> (2011). Accessed 18/09/2012
- 49 Neimark, A.V., Coudert, F.o.-X., Triguero, C., Boutin, A., Fuchs, A.H.,
50 Beurroies, I., Denoyel, R.: Structural Transitions in MIL-53 (Cr): View
51 from Outside and Inside. *Langmuir* **27**(8), 4734-4741 (2011)

- 1 Park, K.S., Ni, Z., Côté, A.P., Choi, J.Y., Huang, R., Uribe-Romo, F.J., Chae,
2 H.K., O’Keeffe, M., Yaghi, O.M.: Exceptional chemical and thermal
3 stability of zeolitic imidazolate frameworks. *P. Natl. A. Sci.* **103**(27),
4 10186-10191 (2006)
- 5 Poirier, E., Chahine, R., Bénard, P., Lafi, L., Dorval-Douville, G., Chandonia,
6 P.A.: Hydrogen Adsorption Measurements and Modeling on Metal-
7 Organic Frameworks and Single-Walled Carbon Nanotubes. *Langmuir*
8 **22**(21), 8784-8789 (2006)
- 9 Poirier, E., Dailly, A.: Thermodynamic study of the adsorbed hydrogen phase in
10 Cu-based metal-organic frameworks at cryogenic temperatures. *Energy*
11 *Environ. Sci.* **2**(4), 420-425 (2009)
- 12 Purewal, J., Liu, D., Sudik, A., Veenstra, M., Yang, J., Maurer, S., Müller, U.,
13 Siegel, D.J.: Improved Hydrogen Storage and Thermal Conductivity in
14 High-Density MOF-5 Composites. *J. Phys. Chem. C* **116**(38), 20199-
15 20212 (2012)
- 16 Quiñones, I., Guiochon, G.: Derivation and Application of a Jovanovic–
17 Freundlich Isotherm Model for Single-Component Adsorption on
18 Heterogeneous Surfaces. *J. Colloid Interf. Sci.* **183**(1), 57-67 (1996)
- 19 Richard, M.A., Bénard, P., Chahine, R.: Gas adsorption process in activated
20 carbon over a wide temperature range above the critical point.
21 Part 1: modified Dubinin-Astakhov model. *Adsorption* **15**(1), 43-51
22 (2009)
- 23 Rouquerol, J., Rouquerol, F., Sing, K.S.W.: *Absorption by Powders and Porous*
24 *Solids*. Elsevier Science, (1998)
- 25 Rudzinski, W., Everett, D.H.: *Adsorption of gases on heterogeneous surfaces*.
26 Academic Press, (1992)
- 27 Schlichtenmayer, M., Hirscher, M.: Nanosponges for hydrogen storage. *J. Mater.*
28 *Chem.* **22**(20), 10134-10143 (2012)
- 29 Serre, C., Bourrelly, S., Vimont, A., Ramsahye, N.A., Maurin, G., Llewellyn,
30 P.L., Daturi, M., Filinchuk, Y., Leynaud, O., Barnes, P., Férey, G.: An
31 Explanation for the Very Large Breathing Effect of a Metal–Organic
32 Framework during CO₂ Adsorption. *Adv. Mater.* **19**(17), 2246-2251
33 (2007)
- 34 Silvera, I.F.: The solid molecular hydrogens in the condensed phase:
35 Fundamentals and static properties. *Rev. Mod. Phys.* **52**(2) (1980)
- 36 Sips, R.: On the Structure of a Catalyst Surface. *J. Chem. Phys.* **16**(490) (1948)
- 37 Sips, R.: On the Structure of a Catalyst Surface. II. *J. Chem. Phys.* **18**(8) (1950)
- 38 Ströbel, R., Garche, J., Moseley, P.T., Jörissen, L., Wolf, G.: Hydrogen storage by
39 carbon materials. *J. Power Sources* **159**(2), 781-801 (2006)
- 40 Toth, J.: Gas-Dampf-Adsorption an festen Oberflächen inhomogener Aktivitäten.
41 *Acta Chim. Acad. Sci. Hung.* **30** (1962)
- 42 U.S. Department of Energy: Targets for Onboard Hydrogen Storage Systems for
43 Light-Duty Vehicles. In, vol. 2012. (2009)
- 44 Wang, Q., Johnson, J.K.: Computer Simulations of Hydrogen Adsorption on
45 Graphite Nanofibers. *J. Phys. Chem. B* **103**(2), 277-281 (1998)
- 46 Wilson, M.C., Galwey, A.K.: Compensation Effect in Heterogeneous Catalytic
47 Reactions including Hydrocarbon Formation on Clays. *Nature* **243**(5407),
48 402-404 (1973)
- 49 Zhou, L., Yao, J., Wang, Y., Zhou, Y.: Estimation of Pore Size Distribution by
50 CO₂ Adsorption and its Application in Physical Activation of Precursors.
51 *Chin. J. Chem. Eng.* **8**(3), 279-282 (2000)

- 1 Zhou, W., Wu, H., Hartman, M.R., Yildirim, T.: Hydrogen and Methane
- 2 Adsorption in Metal–Organic Frameworks: A High-Pressure Volumetric
- 3 Study. *J. Phys. Chem. C* **111**(44), 16131-16137 (2007)
- 4
- 5